12. Poeaim, A., Poeaim, S., Soytong, K. and Krajangvuthi, T., Genetic diversity of *Ficus carica* L. based on non-coding regions of chloroplast DNA. In 8th International Symposium on Biocontrol and Biotechnology, 2012.
13. Rakshith, D., Santosh, P. and Satish, S., Isolation and characterization of antimicrobial metabolite producing endophytic *Phomopsis* sp. from *Ficus pumila* Linn. (Moraceae). *Int. J. Chem. Anal. Sci.*, 2013, **4**(3), 156–160.
14. Oxelman, B., Lidén, M. and Berglund, D., Chloroplast rps16 intron phylogeny of the tribe Sileneae (Caryophyllaceae). *Plant. Syst. Evol.*, 1997, **206**(1–4), 393–410.
15. Bast, F., Sequence similarity search, multiple sequence alignment, model selection, distance matrix and phylogeny reconstruction. *Nature Protoc. Exchange*, 2013; doi:10.1038/protex.2013.065.
16. Honorio Coronado, E. N., Dexter, K. G., Poelchau, M. F., Hollingsworth, P. M., Phillips, O. L. and Pennington, R. T., *Ficus insipida* subsp. *insipida* (Moraceae) reveals the role of ecology in the phylogeography of widespread Neotropical rain forest tree species. *J. Biogeogr.*, 2014, **41**(9), 1697–1709.
17. Templeton, A. R., Using phylogeographic analyses of gene trees to test species status and processes. *Mol. Ecol.*, 2001, **10**(3), 779–791.
18. Bruun-Lund, S., Clement, W. L., Kjellberg, F. and Rønsted, N., First plastid phylogenomic study reveals potential cyto-nuclear discordance in the evolutionary history of *Ficus* L. (Moraceae). *Mol. Phylogenet. Evol.*, 2017, **109**, 93–104.
19. Fine, P. V., Zapata, F., Daly, D. C., Mesones, I., Misiewicz, T. M., Cooper, H. F. and Barbosa, C. E. A., The importance of environmental heterogeneity and spatial distance in generating phylogeographic structure in edaphic specialist and generalist tree species of *Protium* (Burseraceae) across the Amazon Basin. *J. Biogeogr.*, 2013, **40**(4), 646–661.
20. Alberto, F. J. *et al.*, Potential for evolutionary responses to climate change – evidence from tree populations. *Global Change Biol.*, 2013, **19**(6), 1645–1661.
21. Dalmaris, E., Ramalho, C. E., Poot, P., Veneklaas, E. J. and Byrne, M., A climate change context for the decline of a foundation tree species in south-western Australia: insights from phylogeography and species distribution modelling. *Ann. Bot.*, 2015, **116**(6), 941–952.
22. Mayol, M. *et al.*, Adapting through glacial cycles: insights from a long-lived tree (*Taxus baccata*). *New Phytol.*, 2015, **208**(3), 973–986.
23. Woolbright, S. A., Whitham, T. G., Gehring, C. A., Allan, G. J. and Bailey, J. K., Climate relicts and their associated communities as natural ecology and evolution laboratories. *Trends Ecol. Evol.*, 2014, **29**(7), 406–416.
24. Roberts, D. R. and Hamann, A., Glacial refugia and modern genetic diversity of 22 western North American tree species. *Proc. R. Soc. London, Ser. B*, 2015, **282**(1804), 20142903.
25. Wisz, M. S. *et al.*, The role of biotic interactions in shaping distributions and realised assemblages of species: implications for species distribution modelling. *Biol. Rev.*, 2013, **88**(1), 15–30.
26. Khan, S., Al-Quraainy, F., Nadeem, M. and Tarroum, M., Development of genetic markers for *Ochradenus arabicus* (Resedaceae), an endemic medicinal plant of Saudi Arabia. *Genet. Mol. Res.*, 2012, **11**(2), 1300–1308.

ACKNOWLEDGEMENTS. The study was supported by grant-in-aid 'Research Seed Money' scheme of the Central University of Punjab, Bathinda. We thank the Vice-Chancellor, Central University of Punjab for support. We also thank Dr Pankaj Bhardwaj for support in experimental works and all those who helped in sample collection. R.M. thanks the Indian Council of Medical Research, New Delhi for financial support (JRF).

Received 31 October 2017; revised accepted 30 March 2019

doi: 10.18520/cs/v117/i2/293-298

Magmatic epidote in the Grenvillian granitoids of North Purulia Shear Zone, Chhotanagpur Gneissic Complex, India and its significance

Ankita Basak, Bapi Goswami*, Ananya Singha, Somshubhra Das and Chitta Bhattacharyya

Department of Geology, University of Calcutta, 35, Ballygunge Circular Road, Kolkata 700 019, India

Magmatic epidotes of granitoid pluton from North Purulia Shear Zone, eastern India, are identified by textural and chemical criteria. The accessory sphene, epidote, allanite and magnetite in the granitoid indicate high fO_2 during crystallization. Hornblendes were crystallized between 1.2 and 4.8 kbar, 753°C and 783°C as well as high fO_2 (>Ni–NiO buffer). Preservation of magmatic epidote in pluton emplaced at low pressure is due to rapid magma ascent (>3.1 km/year). Fast upward transportation of parental magma of the pluton took place through extensional voids along the regional shear zone.

Keywords. Granitoids, magmatic epidote, oxygen fugacity, shear zone emplacement.

THE petrological implications of magmatic epidote (mEp) have been petrographically and experimentally demonstrated by several workers[1–4]. The presence of mEp in tonalites and granodiorites suggests that the plutons crystallized under lithostatic pressure >6 kbar (refs 2, 3). Survival of mEp in calc-alkaline granitoids implies rapid upward movement of the magma[4]. Consequently, mEp can be used for estimating crystallization pressure, oxygen fugacity and rate of upward movement of melt. Studies on mEp in the Neoarchaean granitoids of Srinivaspura (Eastern Dharwar Craton) and the Paleoproterozoic Malanjkhand Granitoid (Central India) revealed upward magma migration rate of 27.65 and 0.45 km/year respectively[5,6]. In the present study, mEp is distinguished from secondary epidote based on textural and chemical criteria in the granitoids of Agarpur pluton lying in the North Purulia Shear Zone (NPSZ) of Chhotanagpur Gneissic Complex (CGC) of eastern India. The significance of mEp on emplacement mechanism of granitoids is also discussed.

The ENE–WSW-trending Central Indian Tectonic Zone and CGC mark the Grenvillian collsional zone between the North Indian Block and the South Indian Block[7–9] (Figure 1 *a*). The CGC is mainly composed of granitoid and migmatitic gneisses with older enclaves of para- and ortho-metamorphic rocks[10]. The structural trend of the rocks is E–W with steep northern dip. Younger

*For correspondence. (e-mail: bapigoswami69@gmail.com)

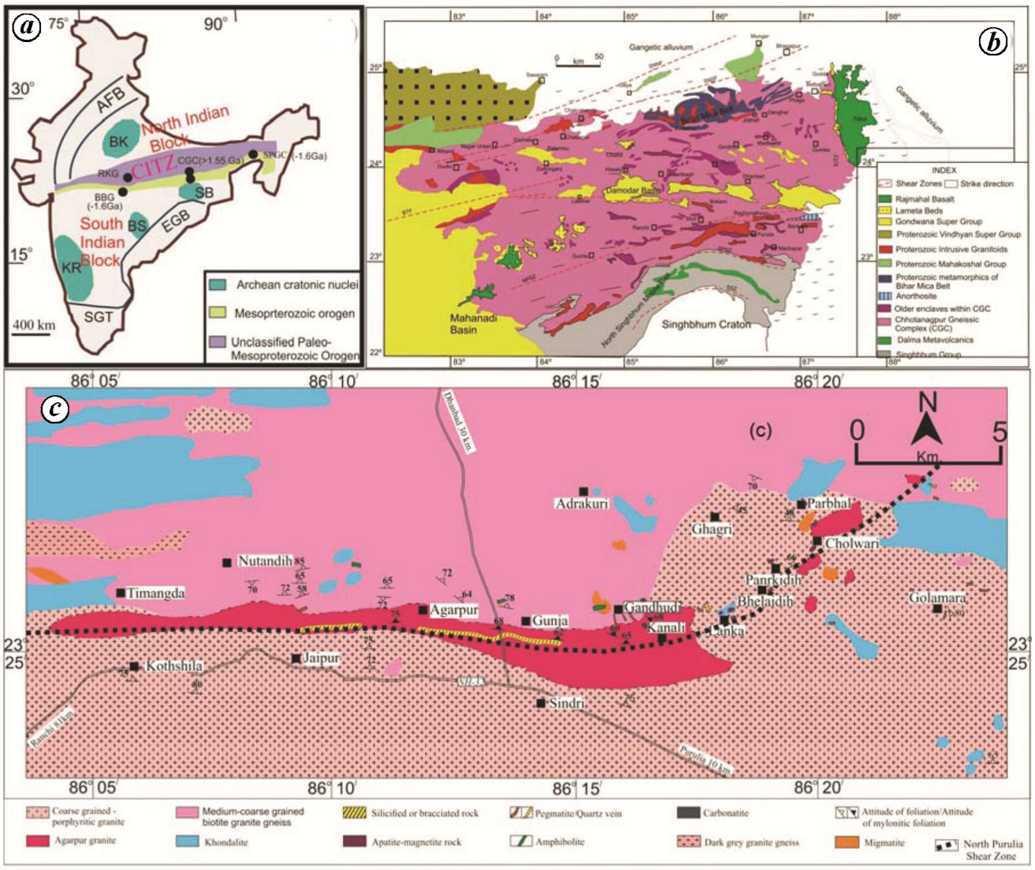

Figure 1. ***a***, Disposition of the major cratonic blocks and tectonic elements within peninsular India. AFB, Aravalli Fold Belt; BBG, Bhandara–Balaghat granulite; CGC, Chhotanagpur Gneissic Complex; EGB, Eastern Ghats Belt; RKG, Ramakona–Katangi granulite; SPGC, Shillong Plateau Gneissic Complex. Archaean cratons: BK, Bundelkhand; BS, Bastar; KR: Karnataka; SB, Singhbhum. SGT, Sourthern Granulite Terrain (modified after Naganjaneyulu and Santosh[24]). ***b***, Generalized geologic map of CGC, showing the distribution of major granitoid plutons (after Mazumdar[25]). SNNF, Son–Narmada North Fault; SNSF, Son–Narmada South Fault; NPSZ, North Purulia Shear Zone; SSZ, Singhbhum Shear Zone. ***c***, Simplified geological map of the area in and around Agarpur, Purulia district, West Bengal, India (modified after Jana and Basu, unpublished).

granitoids, basic and ultrabasic rocks intrude into the granitoid gneisses. The NPSZ in Purulia district, West Bengal, with a trend of E–W to ENE–WSW is a prominent structural feature[9] (Figure 1 *b*). This shear zone is characterized by the occurrence of porphyritic granitoids and lenticular bodies of alkaline rocks (aegirine–riebeckite granite, alkali feldspar–salite granite/syenite, nepheline syenite and minor carbonatite)[11]. Calc-alkaline nature, high oxygen fugacity and high H_2O of the parental magma of Agarpur pluton, lying along the NPSZ suggest the pluton to have been emplaced in a convergent setting[12].

The Agarpur pluton (23 km × 2.5 km; Figure 1 *b*) shows intrusive relation with the country rock comprising migmatitic granite gneisses and porphyritic granitoids. Mylonitic foliation in Agarpur pluton and in the country rocks gives evidence for ductile deformation along the NPSZ. However, locally E–W trending fault breccia develops in the Agarpur pluton (Figure 1 *c*).

The granitoids (alkali feldspar granite, syenogranite and quartz syenite) of Agarpur pluton are coarse-grained, hypidiomorphic and granular. However, distinct preferred orientation of lenticular/ribbon-shaped quartz through the matrix of medium-sized quartzofeldspathic grains defining mylonitic foliation[13] develops along the southern margin of the pluton (Figure 2 *a*). Notwithstanding these textural diversities, mineral assemblages are the same in both the above two textural varieties: K-feldspar (microcline, microcline perthite), quartz, plagioclase (generally albite, acid oligoclase), diopside, hornblende, actinolite, epidote, allanite, sphene, magnetite, apatite and zircon. In hypidiomorphic granitoids aggregates of coarse tabular megacrystic microcline occur with random orientation. Occasionally microcline contain exsolved thin, elongate blebs as well as coarser stringers/veins of albite parallel to its cleavage. Diopside (and hedenbergite) is present as sporadic coarse- to medium-sized skeletal grains containing large inclusions of felsic grains. Amphiboles (both

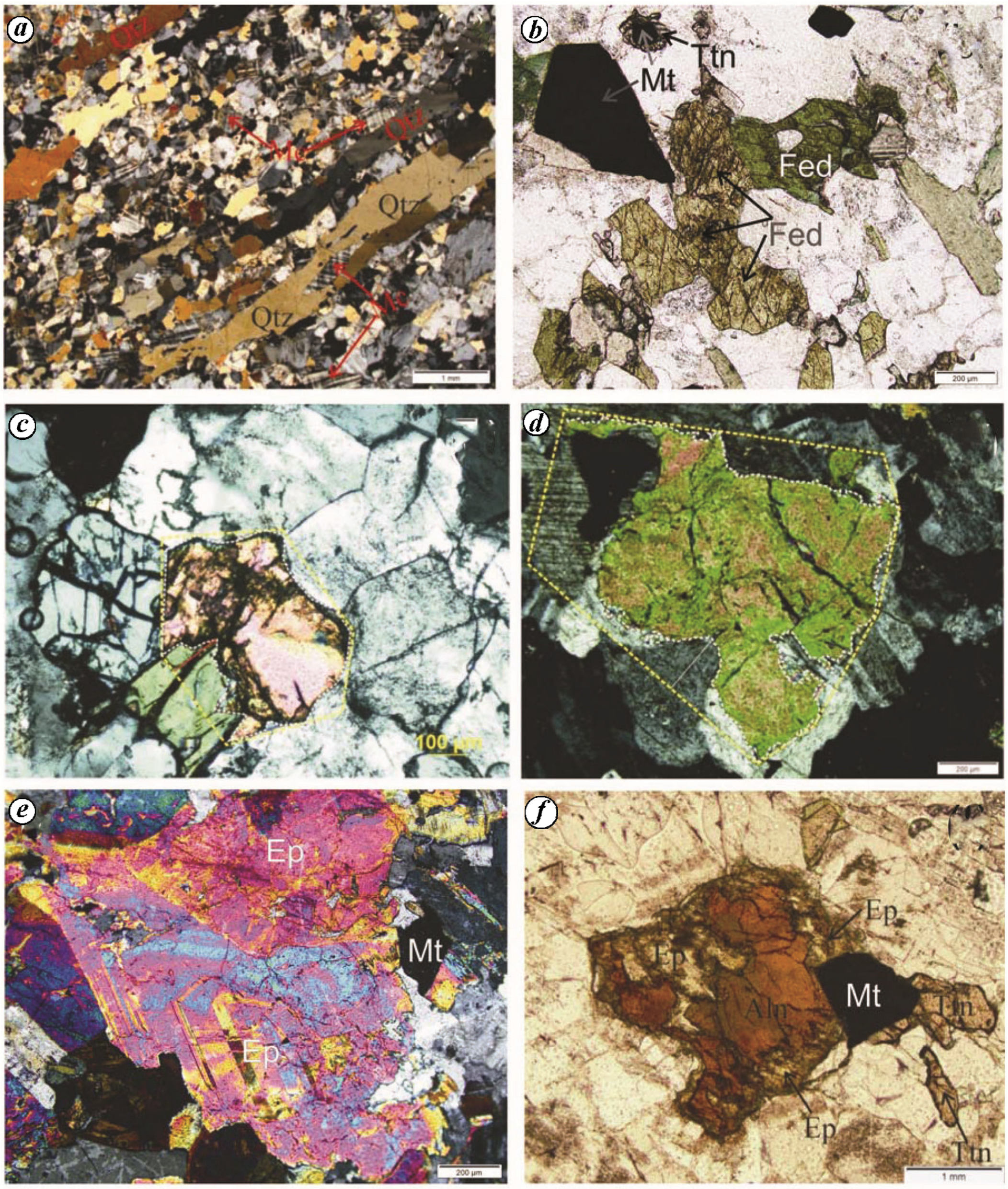

Figure 2. ***a***, Occurrence of thin bands of finer-grained minerals of the matrix in the foliated variety. ***b***, Aggregate of laths of ferroedenite (sample P20B). ***c***, Resorbed outline of epidote in hypidiomorphic granular variety. ***d***, Resorbed epidote showing width of the dissolution zone. ***e***, Magmatic zoning in epidote. ***f***, Epidote rim around allanite.

actinolite and hornblende) occur as (1) aggregates of thin laths (Figure 2 *b*), (2) coarse poikilitic grains enclosing crowds of opaque minerals, feldspar and sphene, (3) thin, irregular stringers along the contact of feldspar and (4) partial replacement of diopside with preservation of relicts of the latter.

Epidote forms medium to coarse subhedral, elongated grains with resorbed boundary at the interspaces of microcline (Figure 2 *c* and *d*). Some epidotes show concentric zoning (Figure 2 *e*), often grading to allanite towards the margin indicating their magmatic origin[3]. Allanite occurs as elongated, irregular or subhedral grains in the interspaces of microclines, and is commonly associated with epidote and magnetite and accompanying radial cracks (Figure 2 *f*). Coarse tabular allanite grains may contain small inclusions of sphene and opaque minerals. From the mineralogical assemblage of sphene + epidote + allanite + magnetite in *Agarpur granitoids*, it is suggested to have crystallized under high oxygen fugacity (>Ni–NiO buffer)[12,14].

Electron probe microanalysis (EPMA) of epidotes and amphiboles of *Agarpur granitoids* was performed using CAMECA SX5 instrument (at the Department of Geology, Institute of Science, Banaras Hindu University,

Table 1. Representative electron micro-probe analyses and cationic calculation of epidote and amphibole of Agarpur granitoid

Sample	P-16	P-16	P-16	P-16	P8B	P8B	P8B	P-18	P-16	P-8B	P-18	S-13	42B	P-13	P-14	P19	P20B
Analysis	11	16	131	127	230	243	242	60	140	246	72	17	30	7	159	168	16
Location	Core	Core	Rim	Core	Core	Rim	Core	Core	Core	Core	Rim	Core	Core	Core	Core	Core	Core
Mineral	Epidote								Magnesio–hornblende					Actinolite		Hastingsite	Ferroedenite
SiO_2	37.03	35.80	37.89	36.74	37.35	37.98	37.99	38.39	46.00	48.35	45.37	49.29	48.35	51.55	54.60	41.38	42.22
TiO_2	0.04	0.00	0.05	0.08	0.00	0.00	0.00	0.00	0.00	0.21	0.13	0.15	0.27	0.28	0.10	0.53	0.44
Al_2O_3	23.15	22.51	19.99	18.45	21.31	20.76	20.71	24.26	7.60	5.14	7.98	3.87	5.04	2.30	1.50	10.45	10.25
Cr_2O_3	0.08	0.00	0.00	0.05	0.00	0.00	0.00	0.00	n.d.	n.d.	n.d.	n.d.	n.d.	n.d.	n.d.	n.d.	n.d.
FeO	12.53	13.17	12.65	14.02	13.56	14.55	15.46	11.06	19.33	16.94	18.13	15.52	14.73	15.26	10.22	21.07	20.67
MnO	0.26	0.17	0.07	0.15	0.46	0.24	0.23	0.00	0.46	0.56	0.18	0.23	0.37	0.69	0.31	0.57	0.14
MgO	0.04	0.07	0.01	0.03	0.00	0.00	0.01	0.02	9.61	11.05	9.66	14.20	14.08	14.54	16.68	7.50	8.09
CaO	22.90	21.86	22.07	20.83	20.66	22.27	22.22	22.70	11.76	11.78	11.71	12.33	12.34	11.18	12.18	11.68	11.18
Na_2O	0.00	0.00	0.01	0.01	0.00	0.01	0.01	0.00	1.23	0.99	1.00	0.84	0.82	0.68	0.52	1.30	1.64
K_2O	0.03	0.02	0.04	0.00	0.03	0.01	0.03	0.03	0.89	0.49	0.57	0.34	0.67	0.30	0.22	1.52	1.35
SrO	0.94	1.21	0.98	1.63	3.73	1.75	1.11	1.12	n.d.	n.d.	n.d.	n.d.	n.d.	n.d.	n.d.	n.d.	n.d.
Total	96.99	94.81	93.76	91.99	97.09	97.56	97.76	97.58	96.87	95.51	94.73	96.77	96.67	96.77	96.30	96.02	95.98
	Number of cations on the basis of 12.5 (O) Cations all Fe^{3+}								Number of cations on the basis of 23 (O) Cations (Fe^{2+}/Fe^{3+} charge balance)								
Si	2.667	2.635	2.810	2.781	2.729	2.817	2.790	2.805	7.010	7.377	7.008	7.283	7.157	7.621	7.941	6.472	6.593
Ti	0.002	0.000	0.003	0.005	0.000	0.000	0.000	0.000	0.000	0.024	0.015	0.017	0.030	0.032	0.010	0.063	0.052
Al	1.966	1.953	1.748	1.646	1.835	1.815	1.792	2.090	1.365	0.925	1.453	0.674	0.879	0.402	0.256	1.927	1.886
Cr	0.004	0.000	0.000	0.003	0.000	0.000	0.000	0.000									
Fe^{3+}	0.764	0.820	0.793	0.898	0.746	0.812	0.854	0.608	0.080	0.000	0.091	0.421	0.384	0.041	0.000	0.305	0.059
Fe^{2+}									2.383	2.161	2.251	1.497	1.439	1.845	1.242	2.452	2.640
Mn	0.016	0.011	0.004	0.010	0.028	0.015	0.014	0.000	0.060	0.073	0.024	0.029	0.046	0.086	0.038	0.076	0.019
Mg	0.004	0.008	0.001	0.004	0.000	0.000	0.001	0.003	2.182	2.514	2.222	3.127	3.107	3.203	3.615	1.749	1.882
Ca	1.768	1.724	1.754	1.689	1.618	1.770	1.748	1.777	1.921	1.926	1.937	1.952	1.957	1.770	1.897	1.957	1.869
Na	0.000	0.000	0.002	0.001	0.000	0.001	0.001	0.000	0.363	0.294	0.300	0.241	0.235	0.196	0.146	0.395	0.497
K	0.002	0.002	0.003	0.000	0.002	0.000	0.002	0.003	0.173	0.094	0.112	0.064	0.127	0.056	0.041	0.304	0.269
Sum	7.965	7.980	7.920	7.942	7.712	8.049	8.066	7.900	15.536	15.388	15.411	15.305	15.362	15.252	15.187	15.699	15.765
Ps	27.974	29.573	31.222	35.289	28.891	30.908	32.272	22.542									
$Fe^{\#}$	0.99	0.99	1.00	1.00	1.00	1.00	1.00	1.00	0.53	0.46	0.51	0.38	0.37	0.37	0.26	0.61	0.59
P (kbar)*									2.8	1.6	3.1	1.2	1.6			4.8	4.6
T (°C)$^{\#}$									783			753	761				
$\Delta NNO^{\#}$												2	2				
H_2O_{melt} (wt.%)#												4	4				

Amphibole formula is after Leake *et al.*[26]

P (kbar) calibration after Mutch *et al.*[20] $^{\#}T$ (°C) ΔNNO and H_2O_{melt} (wt%) calibrations after Ridolfi *et al.*[21].

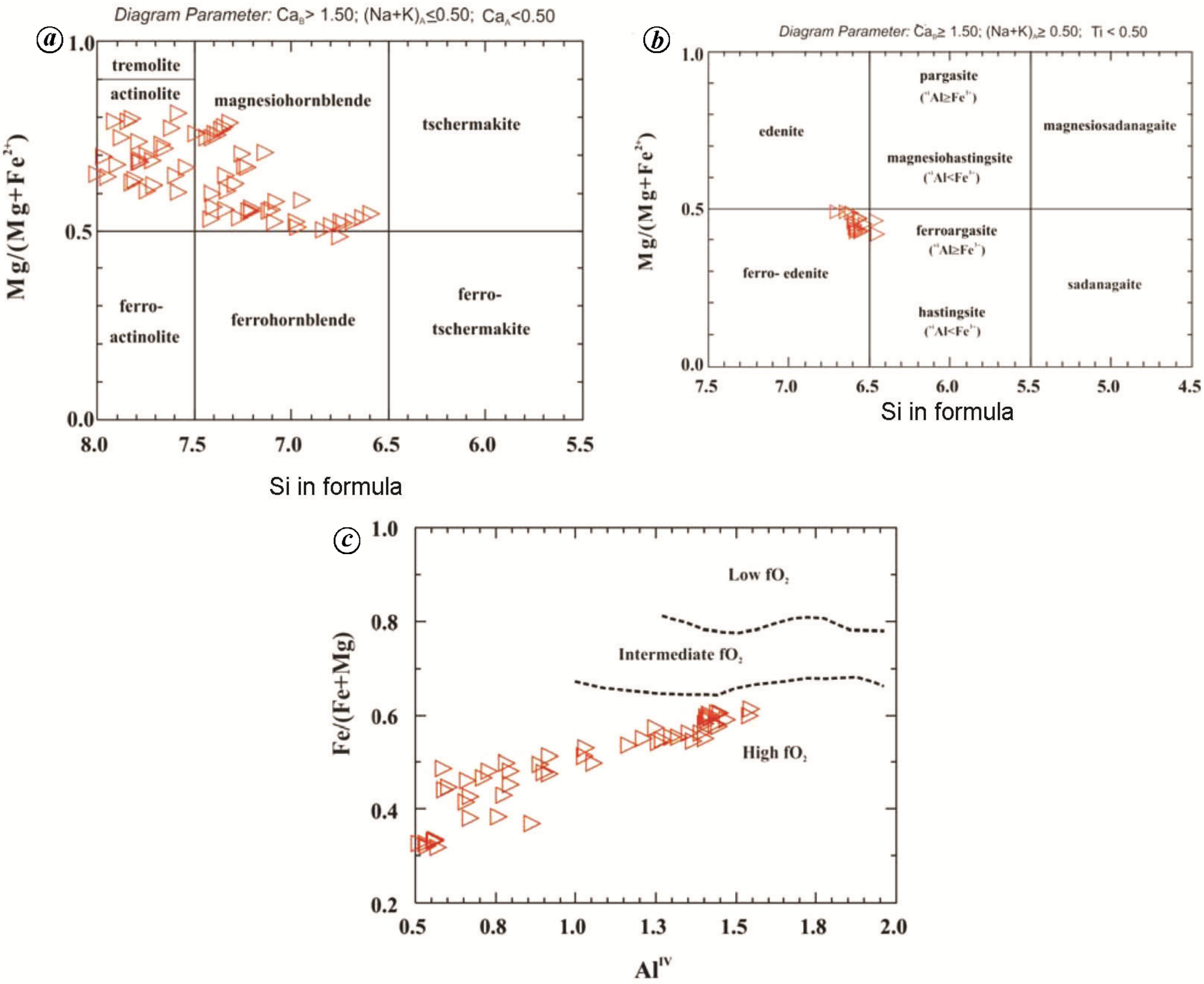

Figure 3. ***a***, ***b***, Classification of amphiboles of Agarpur granitoids according to the scheme of Leake *et al.*[26]. ***c***, Al^{iv} versus Fe/(Fe + Mg) diagram of Anderson and Smith[19] showing the compositional fields of amphiboles crystallized under high, medium and low fO_2 conditions.

Varanasi) and CAMECA SX100 instrument (at the EPMA Laboratory, Central Head Quarter, Geological Survey of India, Kolkata) (Table 1).

The 'pistacite' component (Ps = molar[$Fe^{3+}/(Fe3^{+} + Al) \times 100$]) of magmatic epidotes of granitoid rocks is suggested to range from 20 to 39 (refs 2, 15, 16). The 'pistacite' component (Ps_{22}–Ps_{35}) and low TiO_2 (0.003–0.42 wt%, av. 0.12 wt%) of epidotes from the Agarpur pluton (Table 1) are consistent with their magmatic origin[17]. The epidote composition (Ps_{25}–Ps_{35}; Table 1) corresponds mostly with epidotes from plutons emplaced at or above 3 kbar pressure when fO_2 would lie between nickel–nickel oxide (NNO) and copper–copper oxide (CCO) buffers (25% and 33% Ps in the epidote respectively)[3,18].

All the amphibole species of the studied pluton (Figure 3 *a* and *b*; Table 1) show low Fe/(Fe + Mg) ratio (<0.6; Figure 3 *c*), which suggests crystallization under high fO_2 condition[19]. Al-in-hornblende barometry (calibration of Mutch *et al.*[20]) yields 4.8–1.2 kbar pressure of emplacement for the *Agarpur pluton* (Table 1). The temperature (753–783°C) and ΔNNO (+2) values calculated using the formulations of Ridolfi *et al.*[21] from hornblende composition of the studied rocks are consistent with calc-alkaline nature of the *Agarpur granitoid* magma, as already described elsewhere (Table 1)[12].

The time for partial dissolution of epidote may be given by $t = dz^2/(5 \times 10^{-17})$, where *dz* is the width of the dissolution zone (m)[4]. Several epidote grains in the present study show width of dissolution zone ranging from 80 to 220 μm (Figure 2 *d*), which gives dissolution time between 1.2 and 30 years, and corresponding upward ascent rate between 438 m and 3115 m/year for a decompression from 4.8 to 1.2 kbar pressure as revealed from amphibole chemistry (Table 1). The upward transportation rate of the *Agarpur magma* is comparable (e.g. 455–1800 m/year) to that from epidote-bearing granitoids of northeastern Brazil[22]. The fairly rapid rate of ascent contradicts diapiric emplacement of the *Agarpur pluton*. Remarkable E–W elongation of the *Agarpur pluton* along the NPSZ, presence of both mylonitic and hypidiomorphic granular texture together with the occurrence of associated fault breccia suggest emplacement of the pluton along with shear movement. The rapid upward movement of magma is possible when it would use a pathway along extensional fractures within a regional shear zone[23]. The preservation of mEp, and rapid upward movement of magma together with the linear dyke-like map pattern of the *Agarpur pluton* suggest emplacement of magma along extension-related fractures in the regional NPSZ.

1. Naney, M. T., Phase equilibria of rock-forming ferromagnesian silicates in granitic systems. *Am. J. Sci*., 1983, **283**(10), 993–1033.
2. Zen, E. and Hammarstrom, J. M., Magmatic epidote and its petrologic significance. *Geology*, 1984, **12**, 515–518.
3. Schmidt, M. W. and Thompson, A. B., Epidote in calc-alkaline magmas: an experimental study of stability, phase relationship, and the role of epidote in magmatic evolution. *Am. Mineral.*, 1996, **81**, 462–474.
4. Brandon, A. D., Creaser, R. A. and Chacko, T., Constraints on rates of granitic magma transport from epidote dissolution kinetics. *Science*, 1996, **271**, 1845–1848.
5. Nagar, R. P. and Korakoppa, M. M., Magmatic epidote in the *Neoarchaean granitoids* of Srinivaspura area of Eastern Dharwar Craton and its significance on emplacement mechanism of granitoids. *Curr. Sci.*, 2014, **107**(8), 1321–1324.
6. Pandit, D., Panigrahi, M. K. and Moriyama, T., Constrains from magmatic and hydrothermal epidotes on crystallization of granitic magma and sulfide mineralization in Paleoproterozoic Malanjkhand Granitoid, Central India. *Chem. Erde-Geochem.*, 2014, **74**(4), 715–733.
7. Acharyya, S. K., The nature of Mesoproterozoic Central Indian Tectonic Zone with exhumed and reworked older granulites. *Gondwana Res.*, 2003, **6**(2), 197–214.
8. Bhowmik, S. K., Wilde, S. A., Bhandari, A., Pal, T. and Pant, N. C., Growth of the Greater Indian Landmass and its assembly in Rodinia: geochronological evidence from the Central Indian Tectonic Zone. *Gondwana Res*., 2012, **22**, 54–72.
9. Goswami, B. and Bhattacharyya, C., Petrogenesis of shoshonitic granitoids, eastern India: implications for the late Grenvillian post-collisional magmatism. *Geosci. Front.*, 2014, **5**(6), 821–843.
10. Mahadevan, T. M., *Geology of Bihar and Jharkhand*, Geological Society of India, Bengaluru, 2002, p. 563.
11. Goswami, B. and Bhattacharyya, C., Tectonothermal evolution of Chhotanagpur Granite Gneiss Complex from northeastern part of Puruliya district, West Bengal, eastern India. *Indian J. Geol*., 2008, **80**(1–4), 41–54.
12. Goswami, B., Roy, P., Basak, A., Das, S. and Bhattacharyya, C., Physico-chemical conditions of four calc-alkaline granitoid plutons of Chhotanagpur Gneissic Complex, eastern India: tectonic implications. *J. Earth Syst. Sci*., 2018, **127**(8), 120.
13. Trouw, R. A. J., Passchier, C. W. and Wiersma, D. J., *Atlas of Mylonites – and Related Microstructures*, Springer, 2010, p. 322.
14. Czamanske, G. K. and Wones, D. R., Oxidation during magmatic differentiation, Finnmarka Complex, Oslo Area, Norway; Part 2, The mafic silicates 1. *J. Petrol.*, 1973, **14**(3), 349–380.
15. Tulloch, A., Secondary Ca–Al silicates as low-grade alteration products of granitoid biotite. *Contrib. Mineral. Petrol*., 1979, **69**, 105–117.
16. Johnston, A. D. and Wyllie, P. J., Constraints on the origin of *Archean trondhjemites* based on phase relationships of Nuk gneiss with H_2O at 15 Kbar. *Contrib. Mineral. Petrol.*, 1988, **100**, 35–46.
17. Evans, B. W. and Vance, J. A., Epidote phenocrysts in dacitic dikes, Boulder County, Colorado. *Contrib. Mineral. Petrol*., 1987, **96**, 178–185.
18. Liou, J. G., Synthesis and stability relations of epidote, $Ca_2Al_2FeSiO_3O_{12}OH$. *J. Petrol*., 1973, **14**, 381–413.
19. Anderson, J. L. and Smith, D. R., The effect of temperature and oxygen fugacity on Al-in-hornblende barometry. *Am. Mineral.*, 1995, **80**, 549–559.
20. Mutch, E. J. F., Blundy, J. D., Tattitch, B. C., Cooper, F. J. and Brooker, R. A., An experimental study of amphibole stability in low-pressure granitic magmas and a revised Al-in-hornblende geobarometer. *Contrib. Mineral. Petrol.*, 2016, **171**(10), 85.
21. Ridolfi, F., Renzulli, A. and Puerini, M., Stability and chemical equilibrium of amphibole in calc-alkaline magmas: an overview, new thermobarometric formulations and application to subduction-related volcanoes. *Contrib. Mineral. Petrol*., 2010, **160**(1), 45–66.
22. Sial, A. N., Vasconcelos, P. M., Ferreira, V. P., Pessoa, R. R., Brasilino, R. G. and Morais Neto, J. M., Geochronological and mineralogical constraints on depth of emplacement and ascent rates of epidote-bearing magmas from northeastern Brazil. *Lithos*, 2008, **105**, 225–238.
23. Hutton, D. H. W., Dempster, T. J., Brown, P. E. and Becker, S. D., A new mechanism of granite emplacement: intrusion in active extensional shear zones. *Nature*, 1990, **343**, 452–455.
24. Naganjaneyulu, K. and Santosh, M., The Central India Tectonic Zone: a geophysical perspective on continental amalgamation along a Mesoproterozoic suture. *Gondwana Res*., 2010, **18**(4), 547–564.
25. Mazumdar, S. K., Crustal evolution of Chhotanagpur gneissic complex and the mica belt of Bihar. *Geol. Soc. India, Mem.*, 1988, **8**, 49–83.
26. Leake, B. E. *et al.*, Nomenclature of amphiboles: Report of the Subcommittee on Amphiboles of the International Mineralogical Association Commission on New Minerals and Mineral Names. *Mineral. Mag.*, 1997, **61**(2), 295–321.

ACKNOWLEDGEMENTS. B.G. thanks SERB, DST, Government of India (Sanction no. SB/S4/ES-708/2014, dated 8 October 2014) and University of Calcutta for providing funds. We thank Prof. N. V. Chalapathi Rao and Dr Dinesh Pandit (Department of Geology, Banaras Hindu University, Varanasi) and Dr S. Nandy, Sri S. K. Tripathy and Sri Narahari (Central Head Quarter, Geological Survey of India, Kolkata), for providing EPMA facilities. Constructive comments by an anonymous reviewer and efficient editorial handling by Prof. N. V. Chalapathi Rao are acknowledged.

Received 19 September 2018; revised accepted 20 March 2019

doi: 10.18520/cs/v117/i2/298-303